

Creative Commons DEED Attribution 3.0 Unported (CC BY 3.0)

<https://creativecommons.org/licenses/by/3.0/>

Access to this work was provided by the University of Maryland, Baltimore County (UMBC) ScholarWorks@UMBC digital repository on the Maryland Shared Open Access (MD-SOAR) platform.

Please provide feedback

Please support the ScholarWorks@UMBC repository by emailing scholarworks-group@umbc.edu and telling us what having access to this work means to you and why it's important to you. Thank you.

We are IntechOpen, the world's leading publisher of Open Access books Built by scientists, for scientists

7,000

Open access books available

187,000

International authors and editors

205M

Downloads

Our authors are among the

154

Countries delivered to

TOP 1%

most cited scientists

12.2%

Contributors from top 500 universities



WEB OF SCIENCE™

Selection of our books indexed in the Book Citation Index
in Web of Science™ Core Collection (BKCI)

Interested in publishing with us?
Contact book.department@intechopen.com

Numbers displayed above are based on latest data collected.
For more information visit www.intechopen.com



Lidar Observations in South America. Part I - Mesosphere and Stratosphere

*Eduardo Landulfo, Alexandre Cacheffo,
Alexandre Calzavara Yoshida, Antonio Arleques Gomes,
Fábio Juliano da Silva Lopes, Gregori de Arruda Moreira,
Jonatan João da Silva, Vania Andrioli, Alexandre Pimenta,
Chi Wang, Jiyao Xu, Maria Paulete Pereira Martins,
Paulo Batista, Henrique de Melo Jorge Barbosa,
Diego Alves Gouveia, Boris Barja González, Felix Zamorano,
Eduardo Quel, Clodomyra Pereira, Elian Wolfram,
Facundo Ismael Casasola, Facundo Orte,
Jacobo Omar Salvador, Juan Vicente Pallotta,
Lidia Ana Otero, Maria Prieto, Pablo Roberto Ristori,
Silvina Brusca, John Henry Reina Estupiñan,
Estiven Sanchez Barrera, Juan Carlos Antuña-Marrero,
Ricardo Forno, Marcos Andrade, Judith Johanna Hoelzemann,
Anderson Guimarães Guedes, Cristina Tobler Sousa,
Daniel Camilo Fortunato dos Santos Oliveira,
Ediclê de Souza Fernandes Duarte,
Marcos Paulo Araújo da Silva
and Renata Sammara da Silva Santos*

Abstract

South America covers a large area of the globe and plays a fundamental function in its climate change, geographical features, and natural resources. However, it still is a developing area, and natural resource management and energy production are far from a sustainable framework, impacting the air quality of the area and needs much improvement in monitoring. There are significant activities regarding laser remote sensing of the atmosphere at different levels for different purposes. Among these activities, we can mention the mesospheric probing of sodium measurements

and stratospheric monitoring of ozone, and the study of wind and gravity waves. Some of these activities are long-lasting and count on the support from the Latin American Lidar Network (LALINET). We intend to pinpoint the most significant scientific achievements and show the potential of carrying out remote sensing activities in the continent and show its correlations with other earth science connections and synergies. In Part I of this chapter, we will present an overview and significant results of lidar observations in the mesosphere and stratosphere. Part II will be dedicated to tropospheric observations.

Keywords: lidar, LALINET, aerosols, atmospheric sciences, remote sensing, air quality, environment

1. Introduction

Currently, the world's leading authority on global warming issues is the Intergovernmental Panel on Climate Change (IPCC). The IPCC is a scientific-political organization, created in 1988 by the United Nations (UN), and received the Nobel Peace Prize in 2007 [1, 2]. Since its foundation, the IPCC has issued five reports (Assessment Reports), the first in 1990, the next ones in 1995, 2001, 2007, and 2014. The next report of IPCC is expected for the year 2022. The IPCC reports have reinforced, with growing evidence, that human influence on Earth's climate is incontestable and that the terrestrial climate system's warming is evident [2].

Aerosols, in particular, can alter the most diverse atmospheric processes, significantly affecting weather and climate. For example, they can absorb or scatter specific solar radiation wavelengths and radiation reflected by the Earth's surface [3]. They can also modify the albedo (ability to reflect solar radiation on a given surface) and the lifetime of clouds [4]. A decrease in the albedo of clouds, for example, can lead to less reflection of radiation from the Sun, contributing to possible global warming effects. In this context, it is expected that the aerosol climatological behavior in the Earth's atmosphere and its influence on climate change processes are of paramount importance.

The World Meteorological Organization (WMO) has encouraged the creation and expansion of networks aimed at atmospheric observations, and ground-based lidar networks have acquired great importance, both for atmospheric monitoring and research. Thus, regional lidar networks' development to research the most diverse atmospheric configurations is strategic. The main fields where ground-based lidar measurements can be applied include [5, 6] atmospheric aerosol optical properties, urban aerosols and pollution, dust and biomass burning transportation, and cloud impacts on climate, planetary boundary layer dynamics, and processes of satellite data validation.

In terms of atmospheric structure, ground base lidars cover from the mesosphere down to the troposphere, through the stratosphere, and inspect each atmospheric layer in question. Under this perspective, laser radars' operation began in the early '70s by observing stratospheric aerosols in Brazil and continued with sodium atoms (Na) concentration in the mesosphere. The stratospheric aerosols and ozone studies followed some years later in Argentina [7] and the late '80s in Cuba. By the late '90s and early 2000, the introduction of the lidar for tropospheric studies began.

We intend to summarize the most significant scientific achievements and developments related to ground-based Lidar remote sensing in South America in the next sections. LALINET's most recent efforts in establishing standard protocols of system configurations, quality assurance, measurements, and data processing also will be approached [7–11]. The chapter organization should first follow the studies

performed in the mesosphere, followed by the work devoted to the stratosphere, and then we should show the studies related to the troposphere. These sections will be distributed over many specific studies regarding the scientific drives and methodologies employed.

2. Lidar remote sensing in Latin America: LALINET

The South American continent, encompassing 42% of the Americas, is a region that shelters the most remarkable ecosystems. Among these, we can cite the Amazon Rainforest, which is the largest tropical forest in the world, the Pantanal (or Chaco), one of the UNESCO World Heritage Sites [12], and the Andes, the most extensive mountain chain in the world, and which hold a plethora of active and inactive volcanoes, extending from Venezuela to Patagonia, crossing all the continent from north to south. Patagonia, the continent's southern region, presents many plants and wildlife, mostly endemic. It also houses another UNESCO World Heritage Site: The National Park Los Glaciares, in Santa Cruz, Argentina [12].



Figure 1.
Schematic representation for the location of the LALINET stations in South America. Argentina (AR): 1-) SMN Headquarters (Buenos Aires), 2-) CEILAP Headquarters (Buenos Aires), 3-) Comodoro Rivadavia (Chubut), 4-) Neuquén (Neuquén), 5-) Pilar (Cordoba), 6-) Río Gallegos airport (Santa Cruz), 7-) OAPA Río Gallegos (Santa Cruz), 8-) San Carlos de Bariloche (Río Negro), 9-) San Miguel de Tucumán (Tucumán). Bolivia (BO): 10-) La Paz (La Paz). Brazil (BR): 11-) Manaus (Amazonas), 12-) São Paulo (São Paulo), 13-) Cubatão (São Paulo), 14-) Natal (Rio Grande do Norte). Chile (CH): 15-) Punta Arenas (Magallanes), 16-) Temuco (Cautín). Colombia (CO): 17-) UNAL Medellín (Antioquia), 18-) SIATA Medellín (Antioquia), 19-) Cali (Valle del Cauca). Edited using Google my maps [14].

Developing a regional ground-based lidar network in Latin and South America is of strategic importance: The knowledge rendered by the high-resolution profiles allows the knowledge of a wide variety of atmospheric phenomena to complement satellite observations and other retrievals by diverse ground-based instruments. Unfortunately, the available infrastructure of lidar stations in Latin America is limited in certain aspects. For example, only a few stations operate regularly (contrasted to Europe and North America), stations have different instrument designs, radiosonde launchings are not occurring nearby all stations, and only a reduced number of sun photometers is distributed across the continent [7, 11]. To get around such limitations and consolidate standard protocols of measurements, data acquisition, quality control, and assurance routines, and data analysis, the Latin America Lidar Network, LALINET, was established in 2001, during the First Workshop on Lidar Measurements in Latin America, held in Camagüey, Cuba, in March 2001 [7, 11, 13]. It was recognized as being part of the GAW (Global Atmospheric Watch) Aerosol Lidar Observation Network (GALION) in 2013 [7, 11, 13]. **Figure 1** shows the location of the LALINET stations [14].

The next sections of this chapter will present information about mesospheric, stratospheric, and tropospheric monitoring by LALINET stations and teams around South America and Cuba, plus some significant results. **Table 1** below shows the operational stations and their characteristics. A detailed description of LALINET origin and its evolution is given in Ref. [7]. The Letter of Agreement between LALINET and GAW can be found in Ref. [15].

Country, City, Location Coordinates, Altitude (a.s.l.)	System configuration		
	Instrument	Emits (nm)	Detects (nm)
AR, Buenos Aires, SMN 34.5641 S, 58.4171 W, 10 m	Elastic Polarized	1064, 532, 355	1064, 532 (\parallel , \perp), 355 (\parallel , \perp)
AR, Buenos Aires, CEILAP 34.5553 S, 58.5062 W, 26 m	HSRL	1064, 532, 355	1064, 607, (HSRL, \parallel , \perp), 408, 387, 355 (\parallel , \perp)
AR, Rivadavia, CRD Airport 45.7922 S, 67.4629 W, 48 m	Elastic Polarized	1064, 532, 355	1064, 532 (\parallel , \perp), 355 (\parallel , \perp)
AR, Neuquén, NQN Airport 38.9521 S, 68.1368 W, 266 m	Elastic Polarized	1064, 532, 355	1064, 532 (\parallel , \perp), 355 (\parallel , \perp)
AR, Pilar, OMGP 31.6755 S, 63.8730 W, 332 m	HSRL	1064, 532, 355	1064, 607, 532 (HSRL, \parallel , \perp), 408, 387, 355 (\parallel , \perp)
AR, R. Gallegos, RGL Airport 51.6117 S, 69.3072 W, 17 m	Elastic Polarized	1064, 532, 355	1064, 532 (\parallel , \perp), 355 (\parallel , \perp)
AR, Río Gallegos, OAPA 51.6004 S, 69.3194 W, 19 m	DIAL	355 (Nd:YAG), 308 (Xe:Cl)	387, 355, 347, 332, 308
AR, Bariloche, BRC Airport 41.1473 S, 71.1640 W, 837 m	Raman	1064, 532, 355	1064, 532, 408, 387, 355
AR, S. M. de Tuc., TMO 26.7871 S, 65.2068 W, 485 m	Elastic Polarized	1064, 532, 355	1064, 532 (\parallel , \perp), 355 (\parallel , \perp)
BO, La Paz, UMSA 16.5381 S, 68.0686 W, 3420 m	Scanning Elastic	532	532
BR, Manaus, Embrapa 2.8906 S, 59.9698 W, 80 m	Raman	355	408, 387
BR, São Paulo, IPEN 23.5607 S, 46.7398 W, 764 m	Raman	1064, 532, 355	1064, 532, 530, 408, 387, 355
BR, Cubatão, CEPEMA 23.8865 S, 46.4370 W, 8 m	Mobile Raman	532	532, 607

Country, City, Location Coordinates, Altitude (a.s.l.)	System configuration		
	Instrument	Emits (nm)	Detects (nm)
BR, Natal, UFRN 5.8431 S, 35.2043 W, 20 m	Elastic Polarized	1064, 532, 355	1064, 532 (\parallel , \perp), 355
CH, Punta Arenas, UMAG 53.1344 S, 70.8802 W, 10 m	Raman Polarized	1064, 532, 355	1064, 607, 532 (\parallel , \perp), 408, 387, 355 (\parallel , \perp)
CH, Temuco, UFRO 38.7459 S, 72.6156 W, 108 m	Elastic	532	532
CO, Medellín, UNAL 6.2619 N, 75.5760 W, 1538 m	Elastic	1064, 532	1064, 532
CO, Medellín, SIATA 6.2017 N, 75.5784 W, 1502 m	Elastic Polarized	355	355 (\parallel , \perp)
CO, Cali, CIBioFi-UniValle 3.3770 N 76.5337 W, 982 m	Elastic Polarized	1064, 532, 355	1064 (\parallel , \perp), 532 (\parallel , \perp), 355 (\parallel , \perp)

Details about the contributing teams, measurement protocols, reports, and equipment can be found on the web page <http://www.lalinet.org>. Detection of polarized light in the parallel (\parallel) and perpendicular (\perp) directions are indicated.

Table 1.
LALINET operational stations and their characteristics [7–11].

3. Mesosphere

Meteors enter in the upper atmosphere at very high velocities ($15\text{--}70\text{ km s}^{-1}$), and the collisions with the atmospheric constituents cause flash heating until the particles melt and their chemical elements vaporize. This ablation process is responsible for the layers of metal atoms as Na, K, Fe, Mg, Ca, Si, among others, which occur globally in the mesosphere and lower thermosphere (MLT). This cosmic dust's primary sources are the sublimation of comets as they approach the Sun on their orbits through the solar system and the collisions between asteroids.

Lidar use for the upper stratosphere, mesosphere, and lower thermosphere investigations started in São José dos Campos, Brazil, in 1969 with a ruby laser operated at 694.3 nm. Clemesha and Rodrigues obtained the first aerosol profile using lidar in South America in 1971 [16]. The height range of measurement was 5 to 35 km due to the use of an 8 x 10" receiver mirror. Later were obtained profiles up to 90 km in height using a 48" mirror. In this work, high concentrations of aerosols were observed in the troposphere, a minimum just below the tropopause, around 15 km height, and higher concentrations in the lower stratosphere.

In 1972, when a new "handmade" dye laser became operational (see a Photo of this equipment in **Figure 2**), it was possible to start measurements of the Na layer in the MLT region, using Fabry-Perot interferometers and tuning the laser in the Na D2 line, 5890 Å, with a precision of 0.02 Å [17]. This system enabled the measurement of the mesospheric Na from 75 to 105 km of height [18]. The system continued to be operated regularly for long years obtaining the Na concentration at MLT region with different time and height resolutions, the stratospheric aerosol by Mie Scattering, and the atmospheric density and temperature from 30 to 65 km by Rayleigh scattering. In April 1975, 6 months after the eruption of Volcán de Fuego in Guatemala, a massive increase in aerosol loads was observed in São José dos Campos, which remained in the atmosphere for almost two years [19].

Through Na profiles between 82 and 99 km obtained with the laser beam directed alternately in three positions in the sky, it was possible to estimate the wind's speed in the mesosphere [20, 21]. The velocities vary with height in an oscillatory manner,

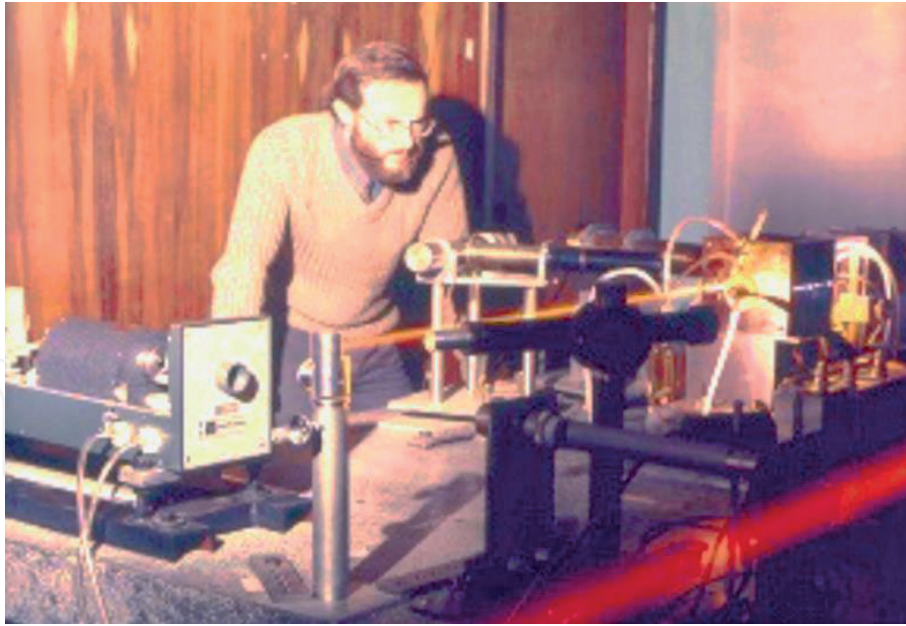


Figure 2.

The handmade dye laser for Na probing (it operates from 1972 to 1992). See also in the picture Dr. Barclay R. Clemesha (in memoriam), the project's head.

with the amplitude increasing with height. These wave-like formations vary slowly with time and might be produced by propagating tides in the atmosphere. These structures' common feature is their downward motion with time, consistent with the upward propagation of gravity wave energy. The more extended periods of oscillations are attributed to tides [22, 23]. Lidar measurements of the stratospheric aerosols enabled the observation of the eruption of El Chichón in México, eight months after in São José dos Campos, Brazil [24]. The transport of aerosols of the Pinatubo eruption was much more rapid and could be seen just 45 days after the eruption [25].

Research involving Na has included the first detection of the so-called Sporadic Sodium Layers [26]. The events occurred more frequently through periods of more significant meteor showers, especially in August. It is common to have sporadic E layers coincident with Na enhancement, which suggests that enhanced layers are generated by the wind shear distortion of Na clouds originated from meteor ablation. A significant result was that the long-lived sporadic layers appear to have a different nature from the short-lived ones. The difference is manifested in the more extensive duration and broader thickness and how the events are correlated with sporadic E layers [27].

In 1992, analyses of the vertical distribution of atmospheric Na layer with lidar showed a long-term trend of the centroid height, which decayed by approximately 700 meters between 1972 and 1987 [28]. However, from 1972 to 2001, the trend was 93 meters per decade. This new result appears dramatically diminishes the possibility of long-term cooling of the upper atmosphere [29].

In 1997 a new technique was developed to measure the Doppler temperature of the atmospheric Na layer by using a two-element birefringent filter together with a 0.2 nm free spectral range Fabry-Perot interferometer to produce a linewidth of about 20 pm. It produced a multi-line signal of the laser, with the lines spacing precisely equal to the separation of D2a and D2b transition of Na. With this assembly, it was possible to obtain the mesosphere's temperature with a 5 K precision, a height resolution of 1 km, and a time resolution of 6 minutes [30, 31]. Lately, in 2004 the lidar was equipped with a new laser, which permitted more precise measurements of the mesopause temperature (see the assembly in **Figure 3**) [32, 33]. Gravity wave's effects on the temperature in the mesopause were also studied [34, 35].

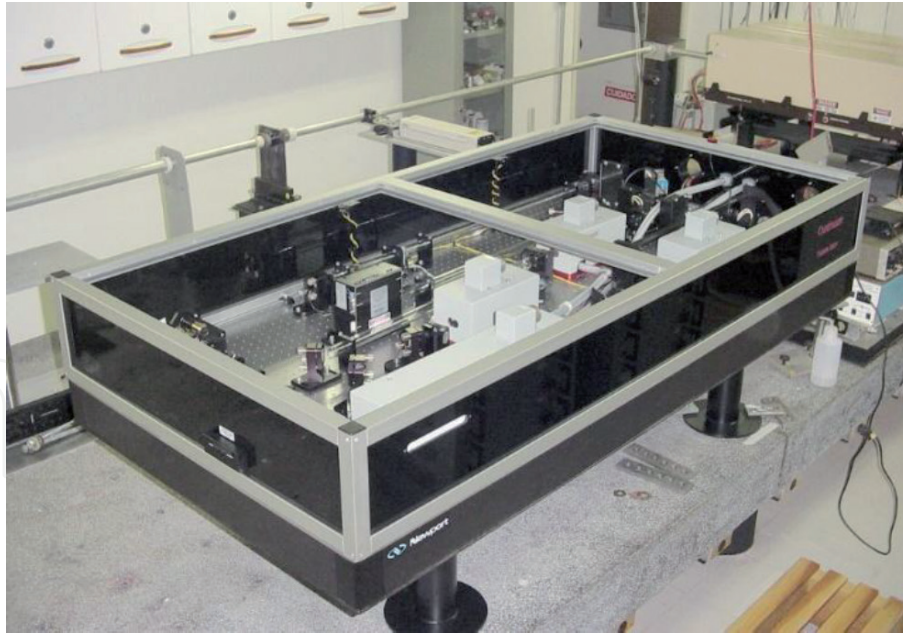


Figure 3.
 Photo presenting the continuum narrowband tunable laser for Na concentration and Mesopause temperatures. It operated at São José dos Campos measuring mesopause temperature from 2007 to 2009 and Na concentration from 2006 to 2016. This photo was taken by Barclay R. Clemesha (in memoriam).

Several mesospheric dynamics studies involving other instruments like photometers, meteor radar, and onboard rocket instruments have been made [23, 36–39]. A mobile lidar has been developed to measure the Na concentration simultaneously with the volume emission profile for the NaD line of airglow in rocket campaigns in the Brazilian equatorial region of Alcântara (2.3728 S, 44.3965 W). An illustrative photo of this system is shown in **Figure 4**. This experiment allowed calculating the branching ratio of the reaction involved in the Na airglow [40].

Along the time, the São José dos Campos lidar underwent many modifications and upgrades. In 1993, the transmitter laser was upgraded with a commercial laser (see its illustration in **Figure 5**). With this upgrade, it was possible to use the Rayleigh signal from the clean atmosphere from 30 to 75 km (below the resonant Na signal) to measure the relative atmospheric density and the absolute temperature. These measurements have been used to study mesospheric temperature general behavior and the effects of atmospheric waves [41]. The long series of measurements have enabled long-term studies of the mesospheric Na, aerosols, and temperatures associated with global change [29, 42, 43]. A dual-beam Na/K lidar was assembled in São José dos Campos, Brazil, to extend the Na layer studies and improve the knowledge about metal layers in the MLT region. This system was installed owing to a cooperative agreement between the National Space Science Center (China) and the National Institute for Space Research (Brazil) in November of 2016.

The lidar uses two laser beams of 589 nm and 770 nm to simultaneously measure Na and K concentrations by the resonant scattering at MLT. The signal-to-noise ratio response allows 3 min time resolution and 96 m of height resolution in the profiles [44]. **Figure 6** shows the Na/K lidar during operation.

It is essential to point out that, up to the present time, this is the unique K lidar system operating in the Southern Hemisphere (SH). For the first time, it was presented the nocturnal and seasonal behavior of K and Na concentrations measured simultaneously at SH [44]. The seasonal variation of these two metals was determined, and it is interesting to note their different behavior even though both are alkali metals and come from meteor ablation. Semiannual variation is observed in both metal concentrations with different maxima: K shows its maxima around the

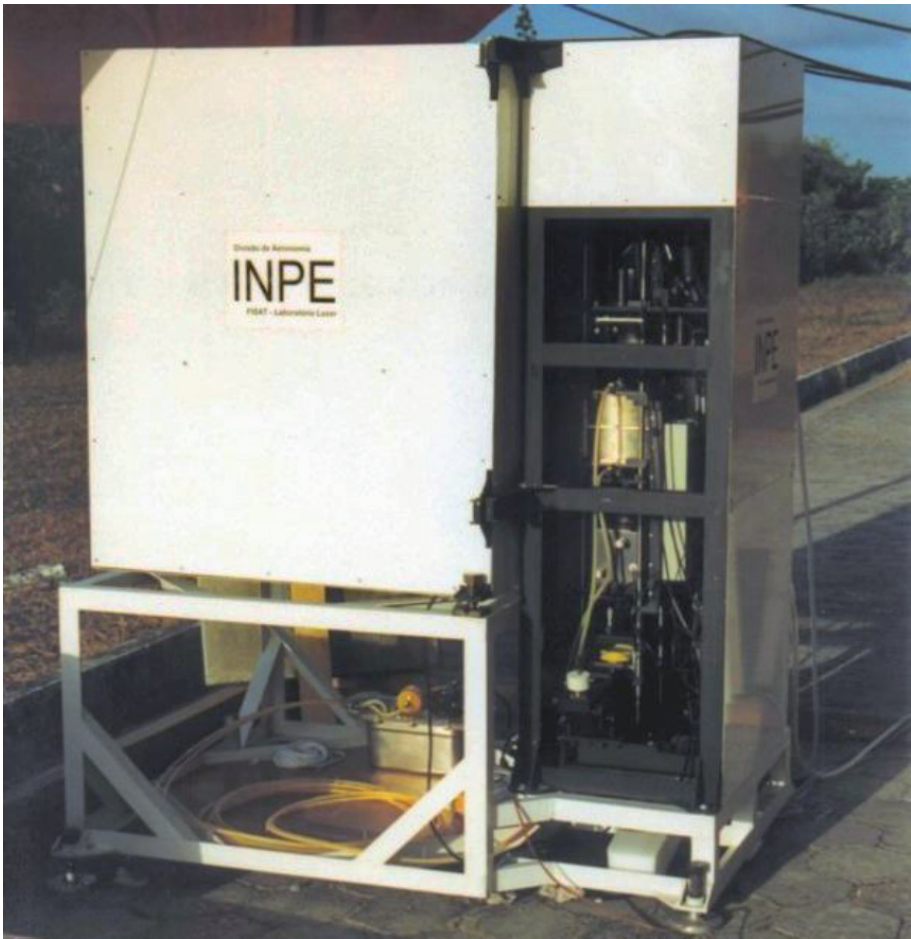


Figure 4.
Photo illustrating the INPE mobile lidar used during rocket campaigns in the Brazilian equatorial region of Alcântara, on 31 may 1992.

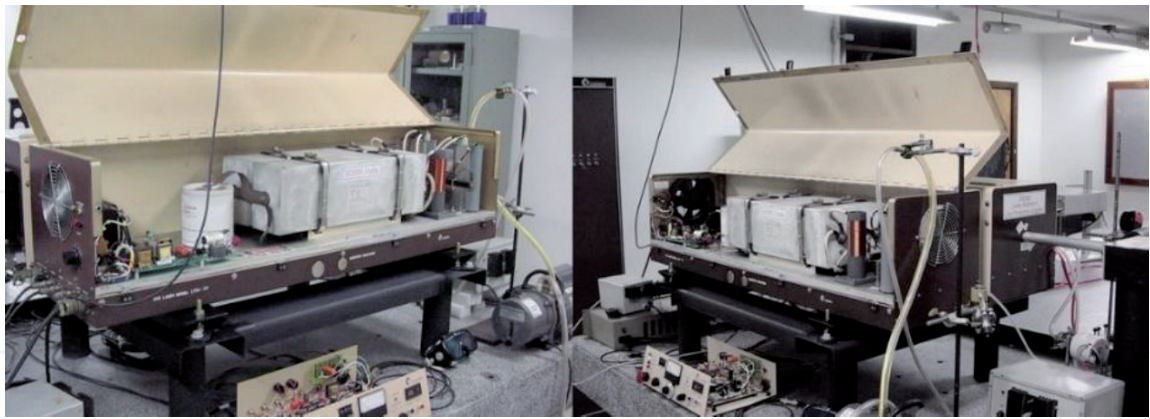


Figure 5.
Photos showing the candela laser system assembled at INPE São José dos Campos in 1993. This system operated between 1993 and 2006—Photos taken by B. R. Clemesha (in memoriam).

solstices more pronounced around June, and Na concentration shows a maximum around May and a broad one centered in September [44]. A plausible interpretation of the different seasonal changes between Na and K concentrations is presented in Ref. [45]. This analysis is based on two points: 1) the neutralization of K^+ ions is particularly favored at low temperatures through summer (North Hemisphere), and 2) cycling between K and its primary neutral reservoir $KHCO_3$ is substantially temperature independent [44]. Unfortunately, the first argument is not significant for this latitude, where the mesopause temperature has not a great summer to winter variation [33].



Figure 6.
Picture showing the dual-beam Na/K lidar located at São José dos Campos, Brazil. The vertical orange beam is at 589 nm for Na scattering and the infrared one at 770 nm for K scattering. This last is not visible in the photo, but the red star indicates the beam position. Liu Zhengkuan took the original photo.

4. Stratosphere

4.1 Historical overview

The first lidar measurements concerning stratospheric aerosols in Latin America were performed in Kingston, Jamaica, between 1964 and 1979 [46]. The lidar system held for these measurements was managed by the University of the West Indies and supported by the US Air Force [47]. Its primary purpose was to investigate the atmospheric profile, measuring molecular scattering. Moreover, the system proved valuable for measurements of stratospheric aerosol layers at wavelength 694 nm [48]. These lidar measurements from Jamaica represented a pioneering role, concomitantly with different research teams, developing lidars' capacities to measure aerosols in the lower stratosphere [49]. Those measurements were also an essential contribution to the stratosphere's early studies in the tropics [50].

In 1969, a new lidar instrument was designed and developed at INPE by Prof. Barclay Clemesha (see Section 3 for details). This equipment's primary objective was to investigate the mesosphere dynamics; besides, stratospheric aerosol measurements were also performed. The first measurements were carried in 1970 at wavelength 694 nm [16], and regular measurements began in 1972 [51]. This project

was responsible for collecting the longest stratospheric aerosol profile measurements in Latin America and the Southern Hemisphere's tropical zone, extending from 1971 to 2016. It includes stratospheric aerosols profiles from the two more significant volcanic eruptions of the XX century second half: the first happened in Mexico on 04 April 1982 (El Chichón), and the second in the Philippines on 14 June 1991 (Mount Pinatubo) [51, 52]. Measurements conducted at INPE between 1972 and 2016 proved the value and the importance of the stratospheric aerosols' long-term monitoring. They have rendered information to understand the stratospheric aerosols layer evolution in the Southern Hemisphere's tropics since the '50s [53].

A Cuban-Soviet scientific cooperation agreement supported the deployment in 1988 of a lidar system designed for stratospheric aerosols measurements at the Camagüey Meteorologic Center in Cuba [54]. The instrument operated intermittently between 1988 and 1997, providing stratospheric aerosols measurements from the Mount Pinatubo eruption in 1991. The 1988–1990 lidar aerosol profiles, at 532 nm, combined with satellite measurements, have been used to study background stratospheric aerosols in the Caribbean [55]. Camagüey Lidar Station (CLS) stratospheric aerosols profiles from Mount Pinatubo also contributed to the study of the radiative impacts of the eruption at regional [56] and global [57] scales. Moreover, the Camagüey lidar database was also used to validate the stratospheric aerosol SAGE II satellite measurements from Mount Pinatubo eruption [58, 59]. Furthermore, it was used to generate an extinction climatology in the UV for correcting Brewer ozone measurements [60].

By 1994 the Laser and Applications Research Center (CEILAP - UNIDEF) in Buenos Aires, Argentina, developed various lidar systems for atmospheric research [7]. One of these devices was designed to measure the atmospheric boundary layer, cirrus clouds, and tropospheric aerosols, operating at wavelength 532 nm [61]. A collaborative study between CEILAP and CLS evaluated how this lidar system could also be used for the higher troposphere and lower stratospheric aerosols research. Upon analyzing two tropospheric aerosols profiles extending into the lower stratosphere, encouraging results were found [62]. In June 2005, another lidar system was designed and installed by CEILAP in Río Gallegos, Patagonia. This instrument's primary goal was performing measurements of stratospheric ozone, tropospheric and stratospheric aerosols, and water vapor. In particular, stratospheric aerosol profiles are used to correct the stratospheric ozone [63].

Western South America is bordered by the Andes, which divides the continent into two distinct regions. In South America, the vast majority of active volcanoes are located in the eastern part of the continent, and ash eruptions are routinely reported throughout the region. The volcanic activity includes periods of ash eruptions and cycling eruptions that spread out over months or even years [64, 65]. Great active volcanoes in South America are Nevado del Ruíz, in Colombia; Cotopaxi, Tungurahua, and Reventador, in Ecuador; Villarrica, Llaima, Nilahue, Lascar, Chaitén, and Calbuco, in Chile; El Misti, Ubinas and Sabancaya, in Peru; Aracar, Copahue, and Planchón-Peteroa in Argentina. There are no reported active volcanoes in Paraguay, Uruguay, Venezuela, Guyana, Suriname, and Brazil [64, 65].

On 22 April 2015, in Chile, the Calbuco volcano erupted and injected a significant amount of ashes and aerosols into the atmosphere [66].

The volcanic aerosol profiles in both the upper troposphere and the lower stratosphere, which originated from the Calbuco volcano eruption in Chile on 22 April 2015, were measured by different lidar stations in South America [7]. It was the first time that LALINET lidar stations, distributed across the continent, could analyze aerosol profiles together during an event. Lidar stations located in Buenos Aires, Comodoro Rivadavia, San Carlos de Bariloche, Neuquén, and Rio Gallegos (all five in Argentina), Concepción (Chile), and São Paulo (Brazil) observed the

aerosols profiles [7, 67]. LALINET stations' capabilities to operate in a coordinated way in case of a volcanic eruption were challenged, highlighting the coordination among LALINET teams.

On 23 April 2015 (one day after the eruption), the lidar system at the University of Concepción measured the aerosols profiles between 5 and 9 km, showing a multilayer structure. Both layers merged at around 7 km, decreasing its intensity and narrowing. The following day 24 April 2015, the two layers registered in the day before at Concepción were detected in the nighttime by the lidar system placed in Buenos Aires, Argentina, in heights varying between 5 and 7 km showing a drowning leaning. The aerosol's multilayer formation was present at both lidar sites when identified for the first time. Lidar measurements conducted at IPEN in São Paulo on 27 April 2015 (five days after the eruption) exhibited aerosols found at an altitude of about 19 km in the stratosphere (**Figure 7**) [66]. Those lidar extinction profiles were confronted with those measured by the Ozone Mapping and Profiler Suite Limb Profiler (OMPS/LP) instrument, revealing promising results [7].

4.2 Differential absorption lidar measurements in Argentina

The behavior of trace constituents in the Earth's upper atmosphere, dictated by diverse physical processes, is of particular interest for the balance of stratosphere and mesosphere. Expressly, ozone has a principal function by absorbing the short-wavelength UV radiation (which might damage life) and keep the radiative budget stable [68]. For those reasons, ozone has been at the focus of the middle atmosphere research effort [69, 70].

Researchers' interest in performing lidar measurements from the southern region of the southern hemisphere dates back to 1995. Researchers from CELAP, together with Prof. Gérard Mégie (who was then head of the *Service d'Aéronomie* in France), considered conducting a campaign to measure ozone profiles using a DIAL (differential absorption lidar) system, in Patagonia, Argentina [71]. The configuration and installation of the lidar system began as a collaboration linking the two institutions. For the DIAL technique, two laser wavelengths are used to measure atmospheric ozone. One wavelength is well absorbed by ozone, while the other not. After the wavelengths travel into the atmosphere and are backscattered

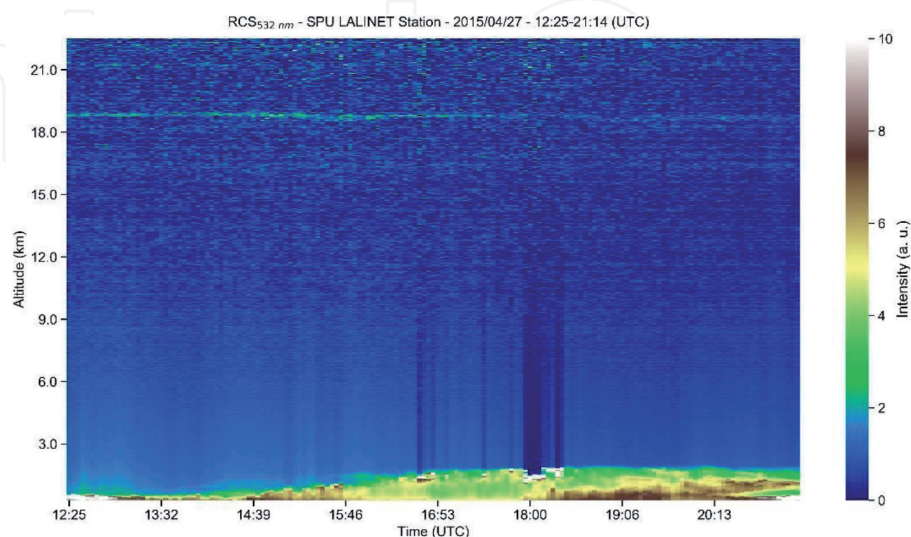


Figure 7. Quick-look of the RCS at 532 nm measured at SPU Lidar Station on 27 April 2015. The SPU Lidar Station is installed at the Center for Lasers and Applications of the nuclear and energy research institute (CELAP/IPEN) in São Paulo. The signal between 18 km and 20 km shows aerosols originating from the Calbuco volcano eruption on 22 April 2015, in Chile.

to two receivers, it is possible to make a ratio of the measurements, allowing direct determination of the ozone concentration as a function of range.

The instrument became operational in 1997 in Villa Martelli, Buenos Aires, where the headquarters of CEILAP is located. The initial version had only one telescope, which was 50 cm in diameter. It operated successfully until 2002. Later, the number of telescopes was increased to four, and a spectrometer was added. The apparatus was fine-tuned at the Villa Martelli headquarters.

The *Service d'Aéronomie* loaned the equipment's electronic project and a container, which had already been used in the Arctic. However, financing was still an issue. Fortunately, since 1999, CEILAP has cooperated with the Tohoku Institute of Technology in Sendai, Japan. The Japan International Cooperation Agency (JICA) supported the south's entire measurement campaign. It further contributed to acquiring a new Nd:YAG laser, which is imperative to the DIAL instrument. In this way, the SOLAR (stratospheric ozone lidar of Argentina) campaign started in June 2005 [72].

The campaign's feasibility study was conducted, considering the nocturnal cloud cover over four towns in Argentine Patagonia. The data were compared with those corresponding to days when the Antarctic polar vortex crosses over these towns.

Different tracers were also considered, such as the total ozone column values measured by total ozone mapping spectrometry, the equivalent latitude method, and the potential vorticity maps calculated for the mid-stratosphere, according to studies carried out in collaboration with the Service d'Aéronomie in France and the National Institute for Environmental Studies in Japan.

The city of Río Gallegos region met the necessary conditions for the measurements. It is located at 2612 km from Buenos Aires, on the River Gallegos estuary banks, and has 140,000 inhabitants. Like other cities in southern Argentina and Chile, Río Gallegos is reached by the ozone hole's edge during the austral spring. However, compared with its counterparts, it has a more significant number of clear nights or nights with less than one-eighth cloud cover, which means more opportunities for making measurements with the ozone DIAL. Río Gallegos also hosts the National University of Southern Patagonia, whose staff could participate in the campaign, and is near to Punta Arenas, Chile, where another research group has used a Brewer instrument to make ozone measurements, in cooperation with Brazilian researchers. On 10 June 2005, the team set off overland for Río Gallegos in two trucks that traveled 2612 km from Buenos Aires to the Military Air Base in Río Gallegos, where a mobile laboratory was set up. The base is located 18 km from the center of the town [72, 73].

A Xe:Cl excimer laser emission at 308 nm is employed for the absorbed wavelength in the DIAL technique, and an Nd:YAG laser at 355 nm third harmonic line is employed as the reference wavelength. Six channels are used for signal acquisition [72]. Four of them detect the emitted wavelengths' elastically backscattered signal (high energy mode for the higher altitude ranges, attenuated energy for the lower ranges), and two correspond to the Raman wavelengths [72]. The CEILAP's DIAL instrument setup is shown in **Figure 8**, and its full description can be found in Ref. [10].

The CEILAP Lidar Division, in cooperation with other national and international institutions, has organized the SOLAR (Stratospheric Ozone Lidar of Argentina) Campaign as a part of environmental investigations in the Southern Hemisphere [72]. This campaign's objective was to monitor different atmospheric constituents using remote sensing techniques, mainly related to lidar, in Argentina's southern part. The most critical and complex instrument involved in this campaign is a differential absorption lidar capable of producing precise and accurate stratospheric ozone profiles [72, 73].

The most substantial decrease of the ozone column over Río Gallegos through the 2005 spring was observed on 8 October, with a total ozone column of 196 DU

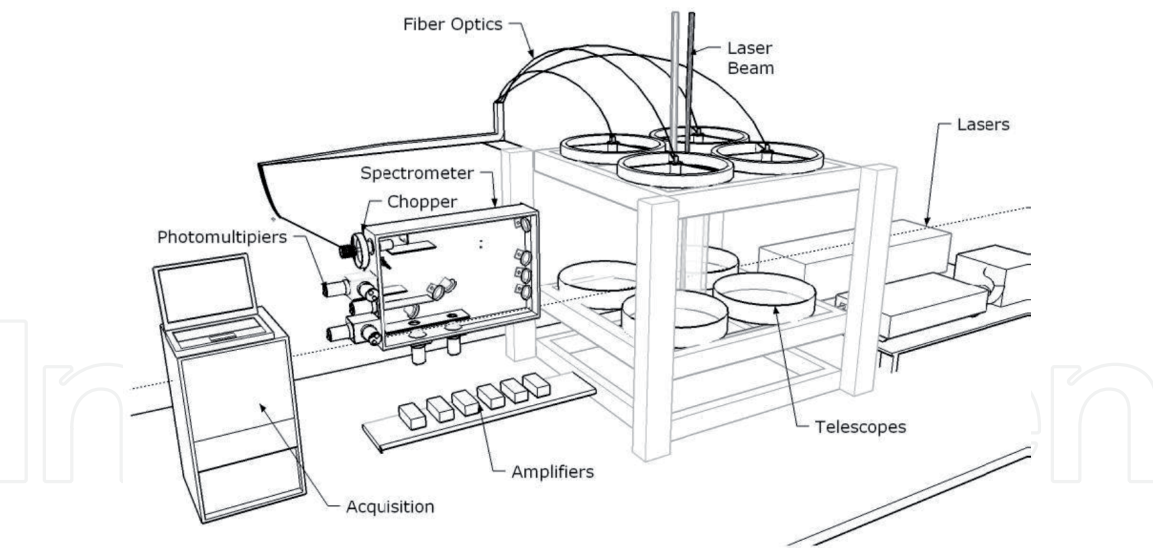


Figure 8.
Experimental setup of differential absorption lidar (DIAL) developed at CEILAP.

estimated from integrating an ozone profile based on the lidar measurement and the US Standard 1976. This value expresses a decrease of 45% in the total ozone column concerning the mean total ozone value outside the ozone hole for this month (about 350 DU). **Figure 9** shows the measured lidar profile on this day (dashed line), together with the ozone profile measured on 17 October (dotted line), which corresponds to standard ozone conditions outside the ozone hole (about 357 DU). The figure also shows the climatologic profile (black line) from the SAGE II measurements, which corresponds to the mean of the ozone measurements outside the ozone hole for the 1995–2004 period.

From the full set of lidar measurements, were selected 37 lidar profiles that match the HRLS profiles. The monthly mean lidar profiles were confronted with similar profiles measured by the High-Resolution Dynamics Limb Sounder (HIRDLS) device onboard the NASA-Aura satellite. The collocation criteria for selecting satellite data were set using a distance of up to 500 km from site measurement and a temporal selection of about twelve hours for the measurement time.

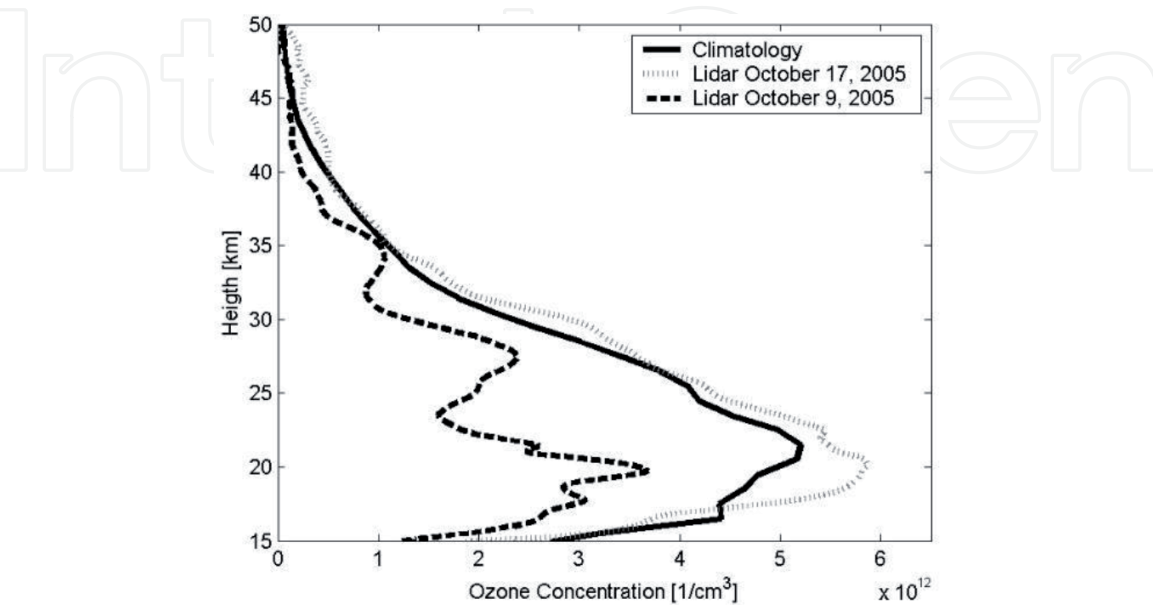


Figure 9.
Lidar ozone profile inside (dashed line) and outside (gray dotted line) ozone hole in Río Gallegos. Climatologic profile for October from SAGE II data (black line) [74].

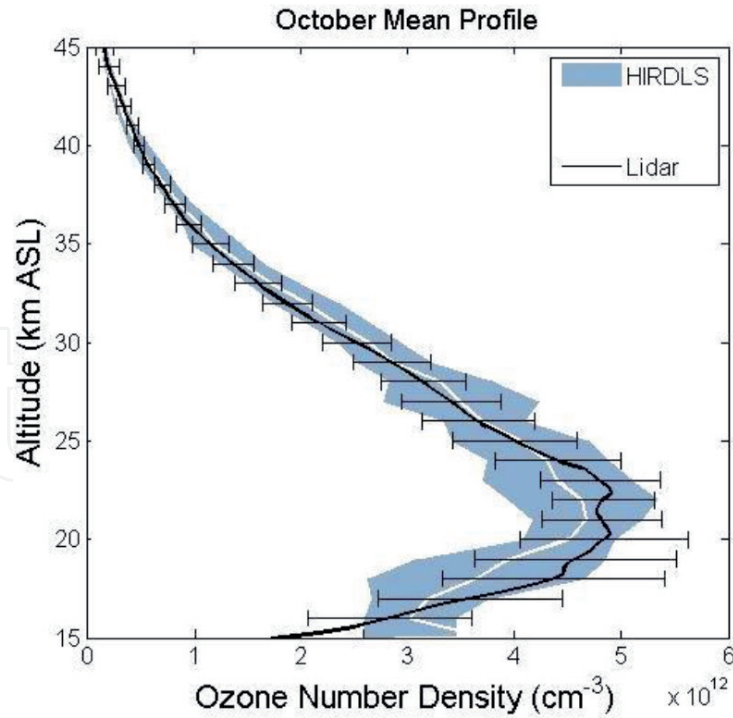


Figure 10.

Mean lidar profile (black line - error bar corresponds to ± 1 std) and mean HIRDLS (white line) ± 1 std. (shadow area) for October.

The mean stratospheric ozone lidar profile for October in Río Gallegos is shown in **Figure 10**. For comparison, the same quantity from satellite data is included.

In general, good agreement between lidar and satellite data was found (inside the statistical error bar, with a relative difference of around 10%). The maximum disagreement between lidar and satellite data was observed in August mean profiles around 30 km. For October, the agreement was better than 10% above the ozone peak concentration. In general, it was observed that the variability of lidar profile concentrations is higher around the ozone peak, decreasing with height.

Differential Absorption lidar techniques have been demonstrated to be a reliable remote sensing technique to retrieve the stratosphere's ozone profile [73]. Argentina has used DIAL techniques since 1999. In 2005, with French and Japanese researchers' collaboration, the Lidar Division of CEILAP established a new site in Southern Patagonia, the South Patagonia Atmospheric Observatory (OAPA). This device has been part of Network Data for Atmospheric Composition Change (NDACC) since 2008, and the research using its measurements allows the study of ozone hole overpass from South America [75] and the satellite validation in the South Hemisphere. After the SOLAR Campaign, several initiatives were carried out related to stratospheric ozone monitoring in Argentina. For example, the UVO3-Patagonia (2008–2010) and SAVER-Net projects (2013–2018) were the research activities made in collaboration with JICA, and Japanese and Chilean Researchers went more in-depth the observation of ozone in vertical profiles and total ozone column [76].

5. Conclusions

Part I of this chapter offered the opportunity to give a scientific overview of current and past lidar observation activities conducted in South America, with Cuba's participation. This overview spans over almost 50 years of activities and grants how this part of the world is concerned with laser remote sensing of the atmosphere in almost its whole structure: Mesosphere and Stratosphere. This top-down approach

also followed a chronological delivery of results, with the first results coming from the region in the highest portion of the atmosphere (mesosphere), and going downwards to stratospheric, and finally at the tropospheric studies. If, in the first years, these activities started as individual initiatives at different countries and research groups levels, the creation of a federative lidar network, namely LALINET, helped somehow to have more coordinated measurements. Moreover, the implementation of SAVERNET in Argentina and Chile improved how these joint measurements are conducted. The studies conducted in the mesosphere account for one of the most extended time series of lidar data, being of great importance in the Southern Hemisphere. Also, significant results about Na and K concentrations and their variability over almost three decades are available. The studies of ozone concentration in the stratosphere also provided relevant results, unprecedented for this portion of the globe. Part II of this chapter will be dedicated to tropospheric lidar observations.

Acknowledgements

The authors are thankful to the Brazilian Agencies National Council for Scientific and Technological Development (CNPq), Coordination for the Improvement of Higher Education Personnel (CAPES), São Paulo Research Foundation (FAPESP), Brazilian Agricultural Research Corporation (EMBRAPA), and National Institute of Amazonian Research (INPA) LBA Central Office in Manaus. The authors also thank the NASA/AERONET teams, Japan International Cooperation Agency (JICA), the Argentine Agencies National Scientific and Technical Research Council (CONICET), National Agency for the Promotion of Research, Technological Development and Innovation (ANPCyT), the Argentine National Defense University (UNDEF), UNDEFI and PID-UTN Projects, the Ministry of Defense of Argentina, and the French National Centre for Scientific Research (CNRS). Also, to all NASA's technical personnel, the Argentine Institute of Scientific and Technical Research for Defense (CITEDEF), and the Argentine National Meteorological Service (SMN), who have kept the solar photometers in operation, and especially to Raúl D'Elia. The authors wish to acknowledge the entire NASA CALIPSO and MODIS (AQUA/TERRA) teams, the NOAA Air Resources Laboratory, for providing the HYSPLIT transport and dispersion model and the READY website, ESA/EOM projects teams, the Suomi NPP (National Polar-orbiting Partnership) Mission teams, and the Sentinel 5-P TROPOMI team. The authors also acknowledge the financial support from CIBioFi, the Colombian Science, Technology, and Innovation Fund-General Royalties System (Fondo CTeI-Sistema General de Regalías), and Gobernación del Valle del Cauca. The authors acknowledge the China-Brazil Joint Laboratory for Space Weather (CBJLSW) for Supporting this Book Chapter. Vania F. Andrioli would like to thank the CBJLSW and the National Space Science Center (NSSC) of the Chinese Academy of Sciences (CAS) for supporting her postdoctoral fellowship. The authors from the Universidad de Magallanes would like to acknowledge the financial support of the Japan Science and Technology Agency (JST) / Japan International Cooperation Agency (JICA), the Science and Technology Research Association for Sustainable Development (SATREPS) through the SAVERNet project; and the Program FONDECYT of the Chilean National Agency for Research and Development (ANID) through Project FONDECYT 11181335.

Conflict of interest

The authors declare no conflict of interest.

Author details

Eduardo Landulfo^{1*}, Alexandre Cacheffo^{1,2}, Alexandre Calzavara Yoshida^{1,2}, Antonio Arleques Gomes¹, Fábio Juliano da Silva Lopes^{1,3}, Gregori de Arruda Moreira^{1,4,5}, Jonatan João da Silva^{1,6}, Vania Andrioli^{7,8}, Alexandre Pimenta⁷, Chi Wang⁹, Jiyao Xu⁹, Maria Paulete Pereira Martins⁷, Paulo Batista⁷, Henrique de Melo Jorge Barbosa^{10,11}, Diego Alves Gouveia^{10,12}, Boris Barja González¹³, Felix Zamorano¹³, Eduardo Quel¹⁴, Clodomira Pereira^{15,16}, Elian Wolfram^{17,18}, Facundo Ismael Casasola^{15,16,19}, Facundo Orte¹⁸, Jacobo Omar Salvador¹⁸, Juan Vicente Pallotta¹⁸, Lidia Ana Otero^{14,19}, Maria Prieto^{15,16}, Pablo Roberto Ristori¹⁴, Silvina Brusca¹⁴, John Henry Reina Estupiñán^{20,21}, Estiven Sanchez Barrera²⁰, Juan Carlos Antuña-Marrero²², Ricardo Forno²³, Marcos Andrade²³, Judith Johanna Hoelzemann²⁴, Anderson Guimarães Guedes²⁵, Cristina Tobler Sousa²⁴, Daniel Camilo Fortunato dos Santos Oliveira^{26,27}, Ediclê de Souza Fernandes Duarte²⁷, Marcos Paulo Araújo da Silva^{26,27} and Renata Sammara da Silva Santos^{1,24}

1 Center for Lasers and Applications (CELAP), Institute of Energy and Nuclear Research (IPEN), Sao Paulo, Brazil

2 Institute of Exact and Natural Sciences of Pontal (ICENP), Federal University of Uberlândia (UFU), Ituiutaba, Brazil

3 Institute of Environmental, Chemical and Pharmaceutical Sciences (ICAQF), Federal University of São Paulo (UNIFESP), Diadema, Brazil

4 Federal Institute of São Paulo (IFSP), Campus Registro, Sao Paulo, Brazil

5 Institute of Astronomy, Geophysics and Atmospheric Sciences (IAG), University of São Paulo (USP), Sao Paulo, Brazil

6 Center for Exact Sciences and Technologies (CCET), Federal University of Western Bahia (UFOB), Barreiras, Brazil

7 National Institute for Space Research (INPE), São José dos Campos, Brazil

8 China-Brazil Joint Laboratory for Space Weather (NSSC/INPE), São José dos Campos, Brazil

9 State Key Laboratory of Space Weather (SKSW), National Space Science Center (NSSC), Chinese Academy of Sciences (CAS), Beijing, China

10 Physics Institute, University of São Paulo (USP), Sao Paulo, Brazil

11 Physics Department, University of Maryland Baltimore County (UMBC), Baltimore, USA

12 Royal Netherlands Meteorological Institute (KNMI), De Bilt, The Netherlands

13 Department of Mathematics and Physics, University of Magallanes (UMAG), Punta Arenas, Chile

14 Institute of Scientific and Technical Research for Defense (CITEDEF) - UNIDEF (MINDEF – CONICET), Buenos Aires, Argentina

15 Military Geographical Service, National Geographic Institute (IGN), Buenos Aires, Argentina

16 General Directorate of Research and Development of the Argentine Army (DIGID), Buenos Aires, Argentina

17 Argentine National Weather Service (SMN), Buenos Aires, Argentina

18 Laser and Applications Research Center (CEILAP), UNIDEF (MINDEF–CONICET), Buenos Aires, Argentina

19 Argentine National Defense University (UNDEF), Army Engineering Faculty (FIE), Buenos Aires, Argentina

20 Centre for Bioinformatics and Photonics (CIBioFi), Universidad del Valle (UniValle), Cali, Colombia

21 Physics Department, Universidad del Valle (UniValle), Cali, Colombia

22 Department of Theoretical, Atomic and Optical Physics, University of Valladolid (UVA), Valladolid, Spain

23 Department of Physics, Major University of San Andrés (UMSA), La Paz, Bolivia

24 Department of Atmospheric and Climate Sciences (DCAC), Federal University of Rio Grande do Norte (UFRN), Natal, Brazil

25 School of Science and Technology (ECT), Federal University of Rio Grande do Norte (UFRN), Natal, Brazil

26 Polytechnic University of Catalonia (UPC), Barcelona, Spain

27 Graduate Program in Climate Sciences, Federal University of Rio Grande do Norte (UFRN), Natal, Brazil

*Address all correspondence to: landulfo@gmail.com; elandulf@ipen.br

IntechOpen

© 2020 The Author(s). Licensee IntechOpen. This chapter is distributed under the terms of the Creative Commons Attribution License (<http://creativecommons.org/licenses/by/3.0>), which permits unrestricted use, distribution, and reproduction in any medium, provided the original work is properly cited. 

References

- [1] The Intergovernmental Panel on Climate Change. About. Working Groups and Reports. Available from: <http://www.ipcc.ch/>. Accessed 22 September 2020.
- [2] The Nobel Peace Prize, 2020: The Nobel Peace Prize Winners of 2007. Available from: <https://www.nobelpeaceprize.org/Prize-winners/Winners/2007>. Accessed 22 September 2020.
- [3] Haywood, J., Boucher, O., 2000: Estimates of the direct and indirect radiative forcing due to tropospheric aerosols: A review. *Reviews of Geophysics*, v. 38, Issue 4, 513-543. <https://doi.org/10.1029/1999RG000078>.
- [4] Lohmann, U., Feichter, J., 2005: Global indirect aerosol effects: A review. *Atmospheric Chemistry and Physics*, v. 5, Issue 3, 715-737. <https://doi.org/10.5194/acp-5-715-2005>.
- [5] Kovalev, W. A., Eichinger, W. E., 2004: *Elastic Lidar: Theory, Practice, and Analysis Methods*. New Jersey: Wiley-Interscience Publication. John Wiley & Sons, Inc. ISBN: 9780471201717. <https://doi.org/10.1002/0471643173>.
- [6] Weitkamp, C., editor. 2005: *Lidar: Range-Resolved Optical Remote Sensing of the Atmosphere*. Springer Series in Optical Sciences. New York: Springer-Verlag. ISBN: 978-0-387-40075-4. <https://doi.org/10.1007/b106786>.
- [7] Antuña, J. C., Landulfo, E., Estevan, R., Barja, B., Robock, A., Wolfram, E., Ristori, P., et al., 2017: LALINET: The First Latin American–Born Regional Atmospheric Observational Network. *Bull. Amer. Meteor. Soc.*, v. 98, Issue 6, 1255-1275. <https://doi.org/10.1175/BAMS-D-15-00228.1>.
- [8] LALINET, 2014: Report of the inversion unified algorithm working group: I Workshop on Lidar Inversion Algorithms-LALINET. Available from: http://lalinet.org/uploads/Analysis/Concepcion2014/report_1_analysis_workshop.pdf. Accessed 22 September 2020.
- [9] Landulfo, E., Lopes, F. J. S., Moreira, G. A., Marques, M. T. A., Osneide, M., Antuña, J. C., et al., 2016: ALINE/LALINET network status. *EPJ Web of Conferences*, v. 119, 19004. *Proc. 27th International Laser Radar Conference (ILRC 27)*. <https://doi.org/10.1051/epjconf/201611919004>.
- [10] Wolfram, E. A., Salvador, J., D’Elia, R., Casiccia, C., Paes Leme, N., Pazmiño, A., et al., 2008: New differential absorption lidar for stratospheric ozone monitoring in Patagonia, South Argentina. *Journal of Optics A: Pure and App. Optics*, v. 10, Issue 10, 104021. <https://doi.org/10.1088/1464-4258/10/10/104021>.
- [11] Guerrero-Rascado, J. L., Landulfo, E., Antuña, J. C., Barbosa, H. M. J., Barja, B., Bastidas, A. E., et al., 2016: Latin American Lidar Network (LALINET) for aerosol research diagnosis on network instrumentation. *J. Atmos. Sol.-Terr. Phys.*, v. 138-139, 112-120. <https://doi.org/10.1016/j.jastp.2016.01.001>.
- [12] UNESCO, 2020: World Heritage Centre. Latin America and the Caribbean. Available from: <http://whc.unesco.org/en/lac/>. Accessed 29 September 2020.
- [13] Rodriguez, A. R., Antuña, J. C., 2017: Standardizing the determination of the molecular backscatter coefficient profiles for LALINET lidar stations using ERA-Interim Reanalysis. *Óptica Pura y Aplicada*, v. 50, Issue 1, 103-113. <https://doi.org/10.7149/OPA.50.1.49013>.
- [14] Google My Maps, 2020. Map data ©2020 INEGI Imagery ©2020 NASA,

TerraMetrics. South America and LALINET Stations, 1:1000. Edited. Available from: <http://lalinet.org>. Accessed 6 November 2020.

[15] LALINET. Letter of Agreement, 2013: Available from: LALINET website: <http://www.lalinet.org/index.php/Aline/Commitment>. Accessed 29 September 2020.

[16] Clemesha, B. R., Rodrigues, S. N., 1971: The stratospheric scattering profile at 23° South. *Journal of Atmospheric and Terrestrial Physics*, v. 33, Issue 7, 1119-1124. [https://doi.org/10.1016/0021-9169\(71\)90132-2](https://doi.org/10.1016/0021-9169(71)90132-2).

[17] Clemesha, B. R., Kirchhoff, V. W. J. H., Simonich, D. M., 1975: Automatic wavelength control of a flashlamp-pumped dye laser. *Optical and Quantum Electronics*, v. 7, 193-196. <https://doi.org/10.1007/BF00619592>.

[18] Kirchhoff, V. W. J. H., Clemesha, B. R., 1973: Atmospheric Sodium Measurements at 23° S. *Journal of Atmospheric and Terrestrial Physics*, v. 35, Issue 8, 1493-1498. [https://doi.org/10.1016/0021-9169\(73\)90150-5](https://doi.org/10.1016/0021-9169(73)90150-5).

[19] Clemesha, B. R., Simonich, D. M., 1978: Stratospheric Dust Measurements, 1970-1977. *Journal of Geophysical Research*, v. 83, Issue C5, 2403-2408. <https://doi.org/10.1029/JC083iC05p02403>.

[20] Clemesha, B. R., Kirchhoff, V. W. J. H., Simonich, D. M., Batista, P. P., 1981: Mesospheric winds from lidar observations of atmospheric sodium. *Journal of Geophysical Research*, v. 86, Issue A2, 868-870. <https://doi.org/10.1029/JA086iA02p00868>.

[21] Clemesha, B. R., Kirchhoff, V. W. J. H., Simonich, D. M., 1981: Remote measurement of tropospheric and stratospheric winds by ground-based lidar. *Applied Optics*, v. 20, Issue 17, 2907-2910. <https://doi.org/10.1364/AO.20.002907>.

[22] Clemesha, B. R., Kirchhoff, V. W. J. H., Simonich, D. M., Takahashi, H., Batista, P. P., 1980: Spaced lidar and nightglow observations of an atmospheric sodium enhancement. *Journal of Geophysical Research: Space Physics*, v. 85, Issue A7, 3480-3484. <https://doi.org/10.1029/JA085iA07p03480>.

[23] Batista, P. P., Clemesha, B. R., Kirchhoff, V. W. J. H., 1985: Tidal oscillations in the atmospheric sodium layer. *Journal of Geophysical Research*, v. 90, Issue D2, 3881-3888. <https://doi.org/10.1029/JD090iD02p03881>.

[24] Clemesha, B. R., Simonich, D. M., 1983: Lidar observations of the El Chichón dust cloud at 23° S. *Geophysical Research Letters*, v. 10, Issue 4, 321-324. <https://doi.org/10.1029/GL010i004p00321>.

[25] Simonich, D. M., Clemesha, B. R., 1995: Comparison between the El Chichón and Pinatubo aerosol clouds at 23° S. In: XXI IUGG General Assembly, Boulder, Colorado, EUA. <http://www.iugg.org/assemblies/1995boulder/>.

[26] Clemesha, B. R., Kirchhoff, V. W. J. H., Simonich, D. M., Takahashi, H., 1978: Evidence of an extra-terrestrial source for the mesospheric sodium layer. *Geophysical Research Letters*, v. 5, Issue 10, 873-876. <https://doi.org/10.1029/gl005i010p00873>.

[27] Batista, P. P., Clemesha, B. R., Batista, I. S., Simonich, D. M., 1989: Characteristics of the sporadic sodium layers observed at 23 S. *Journal of Geophysical Research*, v. 94, Issue A11, 15349-15358. <https://doi.org/10.1029/JA094iA11p15349>.

[28] Clemesha, B. R., Simonich, D. M., Batista, P. P., 1992: A long-term trend in the height of the atmosphere sodium layer possible evidence for global change. *Geophysical Research Letters*, v. 19, Issue 5, 457-460. <https://doi.org/10.1029/92GL00123>.

- [29] Clemesha, B. R., Batista, P. P., Simonich, D. M., 2003: Long-term variations in the centroid height of the atmospheric sodium layer. *Advances in Space Research*, Oxford, v. 32, Issue 9, 1707-1711. [https://doi.org/10.1016/S0273-1177\(03\)90466-2](https://doi.org/10.1016/S0273-1177(03)90466-2).
- [30] Clemesha, B. R., Jorge, M. P. P. M., Simonich, D. M., Batista, P. P., 1997: A new method for measuring the Doppler temperature of the atmospheric sodium layer. *Advances in Space Research*, v. 19, Issue 4, 681-684. [https://doi.org/10.1016/S0273-1177\(97\)00163-4](https://doi.org/10.1016/S0273-1177(97)00163-4).
- [31] Clemesha, B. R., Veselovskii, I., Batista, P. P., Jorge, M. P. P. M., 1999: First mesopause temperature profiles from a fixed southern hemisphere site. *Geophysical Research Letters*, v. 26, Issue 12, 1681-1684. <https://doi.org/10.1029/1999GL900342>.
- [32] Clemesha, B. R., Simonich, D. M., Batista, P. P., 2010: Mesopause region temperature structure observed by sodium resonance lidar. *Journal of Atmospheric and Solar-Terrestrial Physics*, v. 72, Issues 9-10, 740-744. <https://doi.org/10.1016/j.jastp.2010.03.017>.
- [33] Clemesha, B. R., Simonich, D. M. and Batista, P. P., 2011: Sodium lidar measurements of mesopause region temperatures at 23° S. *Advances in space research*, v. 47, Issue 7, 1165-1171. <https://doi.org/10.1016/j.asr.2010.11.030>.
- [34] Yang, G., Clemesha, B., Batista, P., Simonich, D., 2010: Seasonal variations of gravity wave activity and spectra derived from sodium temperature lidar. *Journal of Geophysical Research*, v. 115, Issue D18, D18104. <http://doi.org/10.1029/2009JD012367>.
- [35] Andrioli, V. F., Batista, P. P., Xu, J., Yang, G., Chi, W., Zhengkuan, L., 2017: Strong temperature gradients and vertical wind shear on MLT region associated to instability source at 23° S. *Journal of Geophysical Research: Space Physics*, v. 122, Issue 4, 4500-4511. <https://doi.org/10.1002/2016JA023638>.
- [36] Clemesha, B. R., Kirchhoff, V. W. J. H., Simonich, D. M., Takahashi, H., Batista, P. P., 1979: Simultaneous observations of sodium density and the NaD, OH (8, 3), and OI 5577-Å, nightglow emissions. *Journal of Geophysical Research*, v. 84, Issue A11, 6477-6482. <https://doi.org/10.1029/JA084iA11p06477>.
- [37] Clemesha, B. R., Batista, P. P., Batista, I. S., 1998: Lidar observations of atmospheric sodium at an equatorial location. *Journal of Atmospheric and Solar-Terrestrial Physics*, v. 60, Issue 18, 1773-1778. [https://doi.org/10.1016/S1364-6826\(98\)00144-8](https://doi.org/10.1016/S1364-6826(98)00144-8).
- [38] Clemesha, B. R., Batista, P. P., 2001: Simultaneous measurements of meteor winds and sporadic sodium layers in the 80-110 km region. *Advances in Space Research*, v. 27, Issue 10, 1679-1684. [https://doi.org/10.1016/S0273-1177\(01\)00238-1](https://doi.org/10.1016/S0273-1177(01)00238-1).
- [39] Clemesha, B. R., Batista, P. P., Simonich, D. M., 2002: Tide-induced oscillations in the atmospheric sodium layer. *Journal of Atmospheric and Solar-Terrestrial Physics*, v. 64, Issues 12-14, 1321-1325. [https://doi.org/10.1016/S1364-6826\(02\)00115-3](https://doi.org/10.1016/S1364-6826(02)00115-3).
- [40] Clemesha, B. R., Takahashi, H., Melo, S. M. L., 1993: A simultaneous measurement of the vertical profiles of sodium nightglow and atomic sodium density in the upper atmosphere. *Geophysical Research Letters*, v. 20, Issue 13, 1347-1350. <https://doi.org/10.1029/93gl01121>.
- [41] Batista, P. P., Clemesha, B. R., Simonich, D. M., 2008: Tidal associated temperature disturbances observed in the middle atmosphere (30-65 km) by a Rayleigh Lidar at 23° S. *Advances*

in Space Research, v. 41, Issue 9, 1408-1414. <https://doi.org/10.1016/j.asr.2006.12.002>.

[42] Deshler, T., Anderson-Sprecher, R., Jäger, H., Barnes, J., Hoffman, D. J., Clemesha, B. R., et al., 2006: Trends in the non-volcanic component of stratospheric aerosol over the period 1971-2004. *Journal of Geophysical Research*, v. 111, Issue D1, D01201. <https://doi.org/10.1029/2005JD006089>.

[43] Batista, P. P., Simonich, D. M., Clemesha, B. R., 2009: A 14-year monthly climatology and trend in the 35-65 km altitude range from Rayleigh Lidar temperature measurements at a low latitude station. *Journal of Atmospheric and Solar-Terrestrial Physics*, v. 71, Issue 13, 1456-1462. <https://doi.org/10.1016/j.jastp.2008.03.005>.

[44] Andrioli, V. F., Xu, J., Batista, P. P., Pimenta, A. A., Resende, L. C. A., Savio, et al., 2020: Nocturnal and seasonal variation of Na and K layers simultaneously observed in the MLT Region at 23°S. *Journal of Geophysical Research: Space Physics*, v. 125, Issue 3, e2019JA027164. <https://doi.org/10.1029/2019JA027164>.

[45] Plane, J. M. C., Feng, W., Dawkins, E., Chipperfield, M. P., Höffner, J., Janches, D., Marsh, D. R., 2014: Resolving the strange behavior of extra-terrestrial potassium in the upper atmosphere. *Geophysical Research Letters*, v. 41, Issue 13, 4753-4760. <https://doi.org/10.1002/2014GL060334>.

[46] Philip, M. T., Alleyne, H., 1985: Lidar observations of the stratospheric aerosol layer over Kingston, Jamaica. *J. Atmos. Sci.*, v. 42, Issue 9, 967-976. [https://doi.org/10.1175/1520-0469\(1985\)042<0967:LOOTSA>2.0.CO;2](https://doi.org/10.1175/1520-0469(1985)042<0967:LOOTSA>2.0.CO;2).

[47] Kent, G. S., Ottway, M., Keenlside, W., Wright, R. W. H., Sandford, M.

C. W., 1972: A study of feasibility of measuring atmospheric densities by using a laser-searchlight technique. AFOSR Report n. 43, Period: April 1964 – June 1971. Contract n. AF AFOSR-616-67. Available from: <https://apps.dtic.mil/dtic/tr/fulltext/u2/741875.pdf>. Accessed 13 October 2020.

[48] Clemesha, B., Kent, G. S., and Wright, W. H., 1966: Laser probing the lower atmosphere. *Nature*, v. 209, 184-186. <https://doi.org/10.1038/209184a0>.

[49] Grams, G., and Fiocco, G., 1967: Stratospheric aerosol layer during 1964 and 1965. *J. Geophys. Res.*, v. 72, Issue 14, 3523-3542. <https://doi.org/10.1029/JZ072i014p03523>.

[50] Turco, R. P., Whitten, R. C., Toon, O. B., 1982: Stratospheric aerosols: Observation and theory, *Rev. Geophys.*, v. 20, Issue 2, 233-279. <https://doi.org/10.1029/RG020i002p00233>.

[51] Simonich D.M., Clemesha B.R., 1997: A History of Aerosol Measurements at São José dos Campos, Brazil (23 S, 46 W) from 1972 to 1995. In: Ansmann A., Neuber R., Rairoux P., Wandinger U., editors. *Advances in Atmospheric Remote Sensing with Lidar*, Springer, Berlin, Heidelberg. https://doi.org/10.1007/978-3-642-60612-0_116.

[52] Simonich, D. M., Clemesha B. R., 1989: Decay of the El Chichón aerosol cloud at 23 S. *J. Geophys. Res.*, v. 94, Issue D10, 12803-12806. <https://doi.org/10.1029/JD094iD10p12803>.

[53] Kremser, S., Thomason, L. W., von Hobe, M., Hermann, M., Deshler, T., Timmreck, C., et al., 2016: Stratospheric aerosol—Observations, processes, and impact on climate. *Reviews of Geophysics*, v. 54, Issue 2, 278-335. <https://doi.org/10.1002/2015RG000511>.

[54] Antuña, J. C., Estevan, R., Barja, B., 2012: Demonstrating the potential for

first-class research in underdeveloped countries: Research on stratospheric aerosols and cirrus clouds optical properties, and radiative effects in Cuba (1988-2010). *Bull. Amer. Meteor. Soc.*, v. 93, Issue 7, 1017-1027. <https://doi.org/10.1175/BAMS-D-11-00149.1>.

[55] Antuña, J. C., Estevan, R., Barja, B., 2005: Características de los aerosoles en la troposfera alta y la estratosfera baja en el Gran Caribe en ausencia de perturbación volcánica. *Revista Cubana de Meteorología*, v. 12, Issue 1, 65-72. (In Spanish). Available from: <http://rcm.insmet.cu/index.php/rcm/article/view/310>. Accessed 13 October 2020.

[56] Estevan, R., Antuña, J. C., 2010: Efecto radiativo de la erupción del Monte Pinatubo sobre Camagüey. *Revista Cubana de Meteorología*, v. 16, Issue 1, 90-98, (In Spanish), 2010. Available from: <http://rcm.insmet.cu/index.php/rcm/article/view/136>. Access 13 October 2020.

[57] Stenchikov, G. L., Kirchner, I., Robock, A., Graf, H-F., Antuña, J. C., Grainger, R. G., Lambert, A., Thomason, L., 1998: Radiative forcing from the 1991 Mount Pinatubo volcanic eruption. *Journal of Geophys. Research*, v. 103, Issue D12, 13837-13857. <https://doi.org/10.1029/98JD00693>.

[58] Antuña, J. C., Robock, A., Stenchikov, G. L., Thomason, L. W., Barnes, J. E., 2002: Lidar validation of SAGE II aerosol measurements after the 1991 Mount Pinatubo eruption. *J. Geophys. Res.*, v. 107, Issue D14, ACL 3: 1-11. <https://doi.org/10.1029/2001JD001441>.

[59] Antuña J. C., Robock, A., Stenchikov, G. L., Zhou, J., David, C., Barnes, J., Thomason, L., 2003: Spatial and temporal variability of the stratospheric aerosol cloud produced by the 1991 Mount Pinatubo eruption. *J. Geophys. Res. Atmos.*, v. 108, Issue D – 20. <https://doi.org/10.1029/2003JD003722>.

[60] Stevermer, A. J., Petropavlovskikh, I., Rosen, J. M., DeLuisi, J. J., 2000: Development of a global stratospheric aerosol climatology: Optical properties and applications for UV. *J. Geophys. Res.*, 105, Issue D18, 22763-22776. <https://doi.org/10.1029/2000JD900368>.

[61] Lavorato, M., Cesarano, P., Quel, E., Flamant, P. H., 2002: A dual receiver-backscatter lidar operated in Buenos Aires (34.6 S / 58.5 W). *Proc. 21th ILRC (International Radar Laser Conference)*, 75-78, Quebec, Canada.

[62] Estevan R., Antuña, J. C., Lavorato, M. B., 2008: Stratospheric aerosols measurements at CEILAP, Argentina: Two case studies. *Opt. Pura Apl.*, v. 41, Issue 2, 101-107. *Proceedings of the IV Workshop of Lidar Measurements in Latin America*. ISSN-e 2171-8814. Available from: https://www.sedoptica.es/Menu_Volumenes/Pdfs/282.pdf. Accessed 13 October 2020.

[63] Salvador, J. O., Wolfram, E., Pallotta, J., Otero, L., D'Elia, R., Quel, E., 2008: Correction of a stratospheric ozone profile using stratospheric aerosols backscatter in Rio Gallegos, Argentina. A case study, *Opt. Pura Apl.*, v. 41, Issue 2, 165-170. Available from: https://www.sedoptica.es/Menu_Volumenes/Pdfs/293.pdf. Access 13 October 2020.

[64] Organization of American States, 1990: Disaster, Planning, and Development: Managing Natural Hazards to Reduce Loss. Report. Washington, D. C. Available from <https://www.oas.org/dsd/publications/Unit/oea54e/oea54e.pdf>.

[65] Sigurdson, H., Houghton, B., McNutt, S., Rymer, H., and Stix, J., editors. *The Encyclopedia of Volcanoes*, 2nd Edition, 2015. Elsevier. Academic Press. ISBN: 9780123859389. <https://doi.org/10.1016/C2015-0-00175-7>.

[66] Lopes, F. J. S., Silva, J. J., Antuña, J. C., Ghassan, T., and Landulfo,

- E., 2019: Synergetic Aerosol Layer Observation After the 2015 Calbuco Volcanic Eruption Event. MDPI. Remote Sensing, v. 11, Issue 12, 195. <https://doi.org/10.3390/rs11020195>.
- [67] Bègue, N., Shikwambana, L., Bencherif, H., Pallotta, J., Sivakumar, V., Wolfram, E., Mbatha, N., Orte, F., Du Preez, D. J., Ranaivombola, M., Piketh, S., and Formenti, P., 2020: Statistical analysis of the long-range transport of the 2015 Calbuco volcanic plume from ground-based and space-borne observations, *Ann. Geophys.*, v. 38, Issue 2, 395-420. <https://doi.org/10.5194/angeo-38-395-2020>.
- [68] Watson, R. T., Geller, M. A., Stolarski, R. S., Hampson, R. F., 1986: Present State of Knowledge of the Upper Atmosphere: An Assessment Report. Processes That Control Ozone and Other Climatically Important Trace Gases. NASA Reference Publication 1162. Available from: <https://ntrs.nasa.gov/citations/19860016439>. Document ID: 19860016439. Accessed 2 November 2020.
- [69] Farman, J., Gardiner, B., Shanklin, J., 1985: Large losses of total ozone in Antarctica reveal seasonal ClO_x/NO_x interaction. *Nature* 315, 207-210. <https://doi.org/10.1038/315207a0>.
- [70] Pazmiño, A., Godin-Beekmann, S., Ginzburg, M., Bekki, S., Hauchecorne, A., Piacentini, R. D., Quel, E. J., 2005: Impact of Antarctic polar vortex occurrences on total ozone and UVB radiation at southern Argentinean and Antarctic stations during 1997-2003 period. *Journal of Geophysical Research: Atmospheres*, v. 110, Issue D3, D03103. <https://doi.org/10.1029/2004JD005304>.
- [71] Mégie, G., Ancellet, G., Pelon J., 1985: Lidar measurements of ozone vertical profiles. *Applied Optics*, v. 24, Issue 21, 3454-3463. <https://doi.org/10.1364/AO.24.003454>.
- [72] Wolfram E. A., Salvador, J., Otero, L., Pazmiño, A., Porteneuve, J., Godin-Beekmann, S., Nakane, H., Quel, E. J., 2005: SOLAR campaign: Stratospheric ozone lidar of Argentina. *Proceedings of SPIE*, v. 5887. Lidar Remote Sensing for Environmental Monitoring VI. 588713. <https://doi.org/10.1117/12.620293>.
- [73] Wolfram, E. A., Salvador, J., D'Elia, R., Casiccia, C., Paes Leme, N., Pazmiño, A., Porteneuve, J., Godin-Beekman, S., Nakane H., Quel, E. J., 2008: New differential absorption lidar for stratospheric ozone monitoring in Patagonia, South Argentina. *Journal of Optics A: Pure and Applied Optics*, v. 10, Issue 10, 104021. <https://doi.org/10.1088/1464-4258/10/10/104021>.
- [74] Wolfram, E. A., Salvador, J., Pallotta, J., D'Elia, R., Otero, L., Godin-Beekmann, S., Pazmiño, A., Nakane, H., Quel, E., 2006: SOLAR Campaign: first results of ozone profile measurements at Río Gallegos (51° 55' S, 69° 14' W), Argentina. The 23rd International Laser Radar Conference (ILRC23), Japan. Available from: https://laser-sensing.jp/ilrc23_CD1a2b3c/ILRC23/4O-4.pdf. Accessed 3 November 2020.
- [75] Wolfram, E. A., Salvador, J., Orte, F., D'Elia, R., Godin-Beekmann, S., Kuttippurath, J., Pazmiño, A., Goutail, F., Casiccia, C., Zamorano, F., Paes Leme, N., Quel, E. J., 2012: The unusual persistence of an ozone hole over a southern mid-latitude station during the Antarctic spring 2009: a multi-instrument study. *Annales Geophysicae*, v. 30, Issue 10, 1435-1449. <https://doi.org/10.5194/angeo-30-1435-2012>.
- [76] Ristori, P., Otero, L., Jin, Y., Barja, B., Shimizu, A., Barbero, A., Salvador, J., Bali, J. L., Herrera, M., Etala, P., Acquesta, A., Quel, E., Sugimoto, N., Mizuno, A., 2018: Saver.net lidar network in southern South America. The 28th International Laser Radar Conference (ILRC 28). EPJ Web Conf., v. 176, 09011. <https://doi.org/10.1051/epjconf/201817609011>.